*Short Communication*

# Photocatalytic and photoelectrochemical production of hydrogen peroxide under acidic conditions in organic p-n bilayer/bismuth vanadate system

*Kosuke Ikezoi[1], Mitsuharu Chisaka[2] and Toshiyuki Abe[1,*]*

[1] Department of Frontier Materials Chemistry, Graduate School of Science and Technology, Hirosaki University, 3 Bunkyo-cho, Hirosaki 036-8561, Japan
[2] Department of Sustainable Energy, Graduate School of Science and Technology, Hirosaki University, 3 Bunkyo-cho, Hirosaki 036-8561, Japan
*E-mail: tabe@hirosaki-u.ac.jp

Because hydrogen peroxide ($H_2O_2$) is utilized as an oxidant in various industries, it is desirable to develop a novel, clean, and energy-saving process for $H_2O_2$ production as an alternative to the current manufacturing method (i.e., the anthraquinone method). In this study, the artificial photosynthesis of $H_2O_2$ (i.e., photocatalytic $H_2O_2$ formation) from water and oxygen was investigated in an acidic medium. Herein, a mixed-valence cobalt(II,III)-oxide-loaded bismuth vanadate and an Au-loaded organic p-n bilayer of zinc phthalocyanine (p-type) and fullerene (n-type) were employed as the oxidation and reduction sites, respectively. Further, the photocatalytic formation of $H_2O_2$ in this system was quantitatively confirmed. Furthermore, $H_2O_2$ formation was investigated under photoelectrochemical conditions, where a bias voltage was applied between the oxidation and reduction sites. The maximum photoenergy conversion efficiency for the $H_2O_2$ production was estimated to be < 0.01% owing to the rate-limiting $H_2O_2$ formation that occurred in the system. Therefore, future research should focus on developing an efficient reduction site to improve the photoenergy conversion efficiency.

## 1. INTRODUCTION

Hydrogen peroxide ($H_2O_2$) has attracted attention in various industries as a clean and environmentally friendly oxidant. The anthraquinone method is typically employed for $H_2O_2$ production [1]. This method involves multistep processes comprising the hydrogenation of 2-anthraquinone, oxidation of 2-anthrahydroquinone, extraction of $H_2O_2$ by organic solvents, and regeneration of the side chains of 2-anthraquinone. However, massive energy consumption and organic waste emissions are

regarded as major problems in the commercialization of $H_2O_2$ preparation using this method [2]. Thus, it is desirable to establish a novel, clean, and energy-saving alternative to the anthraquinone method.

The production of $H_2O_2$ from water ($H_2O$) and dioxygen ($O_2$) belongs to the up-hill reaction type (i.e., $2H_2O + O_2 \rightarrow 2H_2O_2$, $\Delta G° = +117$ kJ·mol$^{-1}$); thus, such a reaction can be expected to proceed through a photocatalytic reaction corresponding to artificial photosynthesis. Recently, numerous number of studies have been conducted on the photocatalytic $H_2O_2$ production under alkaline conditions [3-12]. Except for the noble metals, many transition metal oxides are unstable under acidic conditions (indicated by their Pourbaix diagrams [13]). In other words, very few photocatalysts and co-catalysts are available in acidic media. However, an acidic solution of $H_2O_2$ is long-lasting and stable in relation to its alkaline solution owing to the weakly acidic property of $H_2O_2$ [14]. Furthermore, acidic $H_2O_2$ solutions have a high demand in chemical syntheses because the solution can be utilized as it is [15]. However, photocatalytic studies on $H_2O_2$ production, particularly in acidic media, have not been actively conducted.

In the present study, photocatalytic $H_2O_2$ production was investigated in an acidic medium, as shown in **Scheme 1**. Bismuth vanadate loaded with mixed-valence cobalt(II,III) oxide dispersed in a Nafion membrane ($BiVO_4/Nf[Co_3O_4]$) was utilized as the oxidation site, where $H_2O$ is oxidized to $O_2$. Although $Co_3O_4$ is known to be an unstable co-catalyst in acidic media [16], we recently reported that $BiVO_4/Nf[Co_3O_4]$ works as a stable and efficient photoanode even in an acidic medium with a pH of 2 (i.e., crystal structures: nanoporous $BiVO_4$, monoclinic [17,18]; $Co_3O_4$, hexahedron [19,20]) [21] owing to the utilization of Nf as a support for $Co_3O_4$. An organic p-n bilayer, comprising zinc phthalocyanine (ZnPc, p-type) and fullerene ($C_{60}$, n-type), can be used to induce a photocathodic reaction [22]. The reduction of $O_2$ to form $H_2O_2$ or $H_2O$ can occur through two-electron or four-electron transfer, respectively. Au is recognized to function as a catalyst for the selective formation of $H_2O_2$ from $O_2$ [23,24]; thus, an Au co-catalyst was loaded onto the surface of $C_{60}$ in the organo-bilayer (denoted as ZnPc/$C_{60}$-Au). Consequently, upon visible-light irradiation, the photocatalytic production of $H_2O_2$ was accomplished in an acidic medium (pH = 2) using a system composed of $BiVO_4/Nf[Co_3O_4]$ and ZnPc/$C_{60}$-Au.

## 2. EXPERIMENTAL

Zinc phthalocyanine (ZnPc) was purchased from Tokyo Chemical Industry (TCI) and purified by sublimation prior to use (sublimation conditions: temperature, 530 °C; pressure, ~$2 \times 10^{-2}$ Pa) [25]. Pure $C_{60}$ (> 99.5%, TCI) was used as-received. An indium tin oxide (ITO)-coated glass plate (sheet resistance: 8 Ω·cm$^{-2}$; transmittance: > 85%; ITO thickness: 174 nm) or a fluorine-doped tin oxide (FTO)-coated glass plate (sheet resistance: 12 Ω·cm$^{-2}$; FTO thickness: ~800 nm) was used as a base electrode material (acquired from AGC Inc). The other reagents used in this study were of extra-pure grade.

The ZnPc/$C_{60}$ bilayer was fabricated on the ITO-coated glass plate via vapor deposition (pressure: < $1.0 \times 10^{-3}$ Pa; deposition speed: ~0.03 nm·s$^{-1}$) [22]. ZnPc was first coated on the ITO, followed by $C_{60}$ on top of the ZnPc layer. The deposition of Au onto the organo-bilayer was conducted

under photocathodic conditions, in which the organo-bilayer (effective area: 1 cm$^2$) was subjected to an applied potential of –0.2 V (vs. Ag/AgCl (saturated KCl)) in a sulfuric acid solution (pH = 2) containing $5.0 \times 10^{-4}$ mol·dm$^{-3}$ HAuCl$_4$·4H$_2$O, in air. Photoelectrodeposition was performed using a potentiostat (Hokuto Denko, HA-301) equipped with a function generator (Hokuto Denko, HB-104), a Coulomb meter (Hokuto Denko, HF-201), and an X–Y recorder under an irradiation intensity of approximately 70 mW·cm$^{-2}$. The amount of Au deposited on the C$_{60}$ surface was controlled by monitoring the amount of charge passing through the specimen (i.e., 0.04 C).

According to a previously described procedure by Choi et al. **[17]**, BiVO$_4$ was prepared on the FTO-coated glass plate via the formation of a bismuth oxyiodide (BiOI) intermediate, where a drop of vanadyl acetylacetonate solution was dropped onto the BiOI surface followed by sintering. Co$_3$O$_4$ particles (1 mg), which were synthesized according to a reported method **[26]**, were added to 1 mL of alcoholic 0.5 wt.% Nafion solution and then subjected to ultrasonic irradiation. The mixture solution obtained (100 μL) was dropped onto the BiVO$_4$ surface (effective area: 1 cm$^2$), and subsequently dried at room temperature.

The surface of ZnPc/C$_{60}$-Au was observed using scanning electron microscopy (SEM; JEOL, JSM-7000F). The crystal structure of Au was analyzed by X-ray diffraction (XRD; Rigaku, SmartLab 9kW). The absorption spectrum of the ZnPc/C$_{60}$ bilayer was obtained using a spectrophotometer (PerkinElmer, Lambda 35).

For conducting electrodeposition and measuring the voltammograms and photocurrents for acquiring an action spectrum under potentiostatic conditions, a single-compartment cell, comprising a working electrode, a Pt counter electrode, and an Ag/AgCl reference electrode, was utilized. The light intensity was measured using a power meter (Ophir Japan, type 3A); the typical intensity was determined to be approximately 70 mW·cm$^{-2}$ for each measurement. For the action spectral measurements, the light source was combined with a monochromator (Soma Optics, S-10) to irradiate monochromatic light.
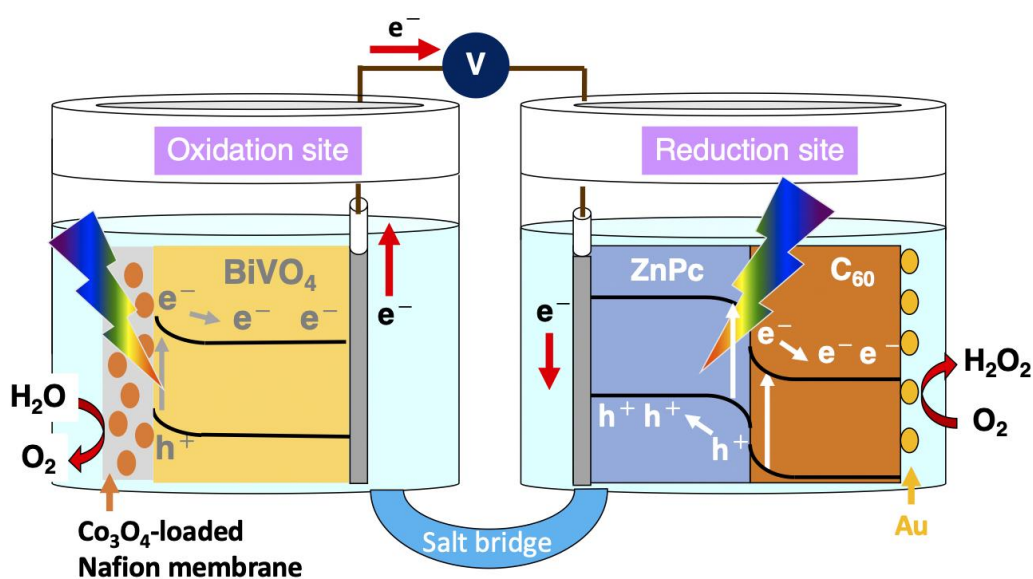


**Scheme 1.** Illustration of photocatalytic cell employed for H$_2$O$_2$ formation.

The photocatalytic and photoelectrochemical formation of $H_2O_2$ were investigated in a twin-compartment cell separated by a salt bridge (**Scheme 1**). To prepare the salt bridge, agar (1.3 g) and $KNO_3$ (4.74 g) were dissolved in hot water (10 mL), and the mixture obtained was poured into the bridging part of the cell and solidified at room temperature. $BiVO_4/Nf[Co_3O_4]$ (oxidation site) and $ZnPc/C_{60}$-Au (reduction site) were placed in each compartment filled with a phosphoric acid solution (pH = 2). Metal halide and halogen lamps were used to irradiate the photoanode and photocathode, respectively. The oxidation product, $O_2$, was quantitatively determined using a gas chromatograph (GL Sciences, GC-3200) equipped with a thermal conductivity detector (column: 5 Å molecular sieve; carrier gas: Ar). Quantification of $H_2O_2$ (the reduction product) was conducted using the following procedures [**27**]: a 30% titanium(IV) sulfate solution (0.5 mL) was added to the electrolyte solution (2.5 mL) at the reduction site; when $H_2O_2$ was present in the solution, a peroxo–titanium complex was formed from a $Ti^{4+}$ ion and an $H_2O_2$ molecule (i.e., $Ti^{4+} + H_2O_2 + 2H_2O \rightarrow H_2TiO_4 + 4H^+$); by measuring the absorption spectrum of the solution, the amount of $H_2O_2$ formed was determined based on the absorbance of the peroxo–titanium complex (absorption maximum: 410 nm; molar absorption coefficient at 410 nm: 674 $M^{-1} \cdot cm^{-1}$).

The incident photon-to-current conversion efficiency (IPCE), light-to-hydrogen peroxide conversion efficiency (LTH), and Faradaic efficiency (F.E.) were determined using the following methods.

The IPCE value was calculated using the following equation:

$$IPCE \ \ (\%) \ = \ ([\ I / e\ ] / [\ W / \varepsilon\ ]) \ \times \ 100,$$

where $I$ is the photocurrent density ($A \cdot cm^{-2}$), $e$ denotes the elementary electric charge (C), $W$ is the light intensity ($W \cdot cm^{-2}$), and $\varepsilon$ is the photon energy of the monochromatic light.

The LTH value was estimated as follows:

LTH (%) = $(\Delta_r G^\circ(H_2O_2)$ [$kJ \cdot mol^{-1}$] × amount of $H_2O_2$ formed [mol] – voltage applied between the anode and cathode [V] × charge passed during $H_2O_2$ formation [C])/(total incident photoenergy irradiated for photoelectrodes [J]) × 100,

where $\Delta_r G^\circ(H_2O_2)$ is +116.78 $kJ \cdot mol^{-1}$, corresponding to the Gibbs free energy for the formation of $H_2O_2$ (1 mol) from $O_2$ and $H_2O$.

The F.E. value was calculated based on the following procedures:

i) During $H_2O_2$ production, the amount of charge passed was measured using a Coulomb meter. The theoretical amount of $H_2O_2$ (or $O_2$) generated was then calculated based on the value obtained.

ii) After performing the photocatalytic or photoelectrochemical reaction, $H_2O_2$ and $O_2$ were quantified by colorimetry and gas chromatography, respectively.

iii) Finally, the F.E. value for $H_2O_2$ (or $O_2$) formation was determined using the following equation:

F.E. (%) = [amount of $H_2O_2$ (or $O_2$) formed]/[theoretical amount of $H_2O_2$ (or $O_2$)] × 100
= [amount of $H_2O_2$ (or $O_2$) formed]/[(amount of charge passed)/($nF$)] × 100,

where *n* is the number of electrons that participated in the formation of the products (i.e., $n = 2$ and 4 for the formation of $H_2O_2$ and $O_2$, respectively) and *F* is Faraday's constant ($9.65 \times 10^4$ C·mol$^{-1}$).

## 4. RESULTS AND DISCUSSION

**Fig. 1(a)** shows the XRD pattern of the Au layer deposited on the $ZnPc/C_{60}$ bilayer. The resulting pattern indicates the formation of polycrystalline Au, which was assigned according to a previous study [28]. **Fig. 1(b)** shows the SEM image of the Au layer deposited on the $C_{60}$ surface in the organo-bilayer, which confirms the formation of fine particles of Au in the order of < 50 nm.
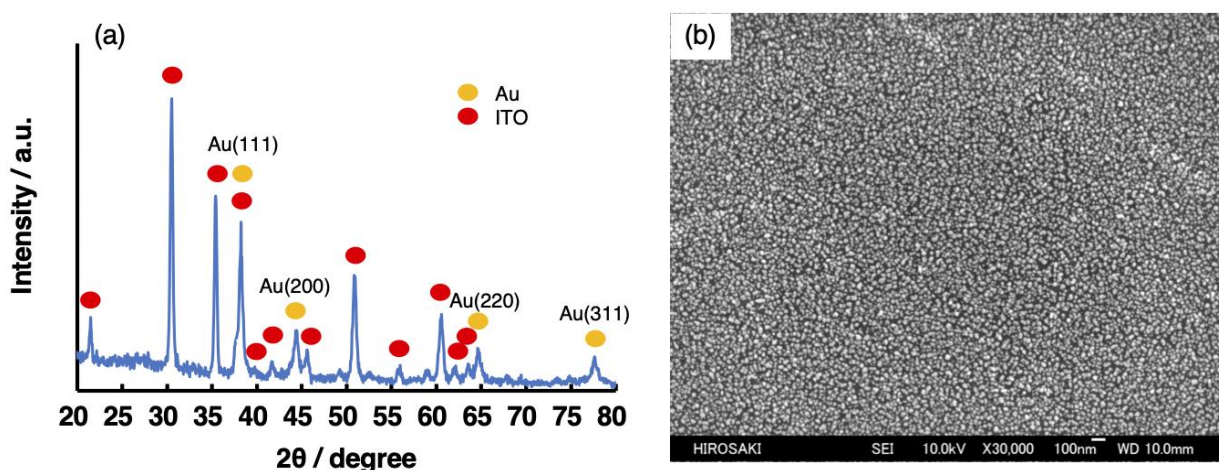


**Figure 1.** (a) XRD pattern and (b) SEM image of $ZnPc/C_{60}$-Au.

**Fig. 2(a)** depicts the voltammograms of $ZnPc/C_{60}$-Au obtained under an $O_2$ atmosphere both under light illumination and in the dark. Accordingly, photocathodic currents were observed owing to the reduction of $O_2$. Moreover, **Fig. 2(a)** shows the voltammogram of $ZnPc/C_{60}$-Au obtained under an Ar atmosphere, where the reduction of $H^+$ to $H_2$ was expected to occur. Based on the photocathodic characteristics of $ZnPc/C_{60}$-Au under both $O_2$ and Ar atmospheres, the organo-photocathode was confirmed to be more active for $O_2$ reduction than for $H^+$ reduction. **Fig. 2(b)** shows that the Au-free organo-bilayer (denoted as $ZnPc/C_{60}$) cannot noticeably induce photocurrents, indicating that the Au co-catalyst is necessary for the reduction of $O_2$, particularly at the organo-bilayer. Furthermore, **Fig. 2(c)** shows the voltammogram of the Au-electrodeposited ITO (denoted as ITO/Au) under an $O_2$ atmosphere in the dark. Based on the results, the $ZnPc/C_{60}$-Au photocathode is superior to the ITO/Au cathode, demonstrating that photoassisted $O_2$ reduction occurs more efficiently in the $ZnPc/C_{60}$-Au photocathode.

As shown in **Fig. 3**, the action spectra for the $ZnPc/C_{60}$-Au photocurrents indicate that the entire visible-light energy, originating from the absorption of both ZnPc and $C_{60}$, is available for $O_2$ reduction. These results are in accordance with our previous studies, where the $ZnPc/C_{60}$ bilayer was employed as a photocathode for $H^+$ reduction [21,22,29,30].
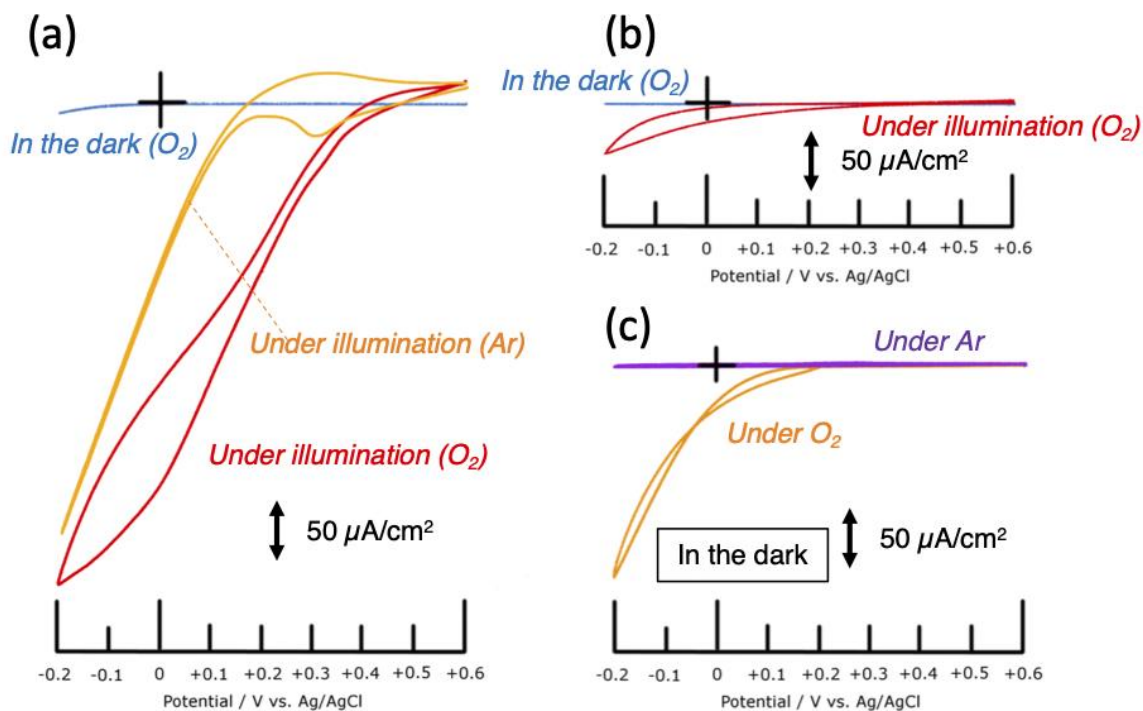
**Figure 2.** (a) Cyclic voltammograms of $ZnPc/C_{60}$-Au obtained under both $O_2$ and Ar atmospheres. Cyclic voltammograms of (b) $ZnPc/C_{60}$ and (c) ITO/Au obtained under $O_2$ atmosphere. Electrolyte solution: an aqueous $H_2PO_4$ solution (pH = 2); scan rate: 20 mV/s; film thickness in (a and b): 75 nm for ZnPc and 125 nm for $C_{60}$; light intensity in (a): 100 mW/cm$^2$; irradiation in (a and b): from back side of ITO-coated face.

**Table 1** Typical photoelectrolysis data for $H_2O_2$ production in system comprising $BiVO_4/Nf[Co_3O_4]$ and $ZnPc/C_{60}$-Au$^a$

|  | Applied voltage/V | Amount of $O_2$/µmol | Amount of $H_2O_2$/µmol | Note |
|---|---|---|---|---|
| Entry 1 | 0 | 0.153 | 0.353 | |
| Entry 2 | 0.1 | 0.489 | 1.03 | |
| Entry 3 | 0.2 | 0.601 | 1.31 | |
| Entry 4 | 0.3 | 0.720 | 1.37 | |
| Entry 5 | 0.4 | 0.778 | 1.61 | |
| Entry 6 | 0.2 | — | 1.21 | Applied voltage: 0.2 V; concentration of electron donor ($H_2O_2$) at the oxidation site: 20 mM (pH = 2) |
| Entry 7 | 0.2 | 3.77 | — | Applied voltage: 0.2 V; concentration of electron acceptor ($Fe^{3+}$) at the reduction site: 20 mM (pH = 2) |

$^a$Film thickness: 75 nm for ZnPc and 125 nm for $C_{60}$; electrolyte solution: aqueous $H_3PO_4$ solution (pH = 2); reaction time: 3 h. Irradiation was conducted from back side of ITO (or FTO)-coated face (light intensity for $BiVO_4/Nf[Co_3O_4]$: 70 mW·cm$^{-2}$; light intensity for $ZnPc/C_{60}$-Au: 70 mW·cm$^{-2}$).
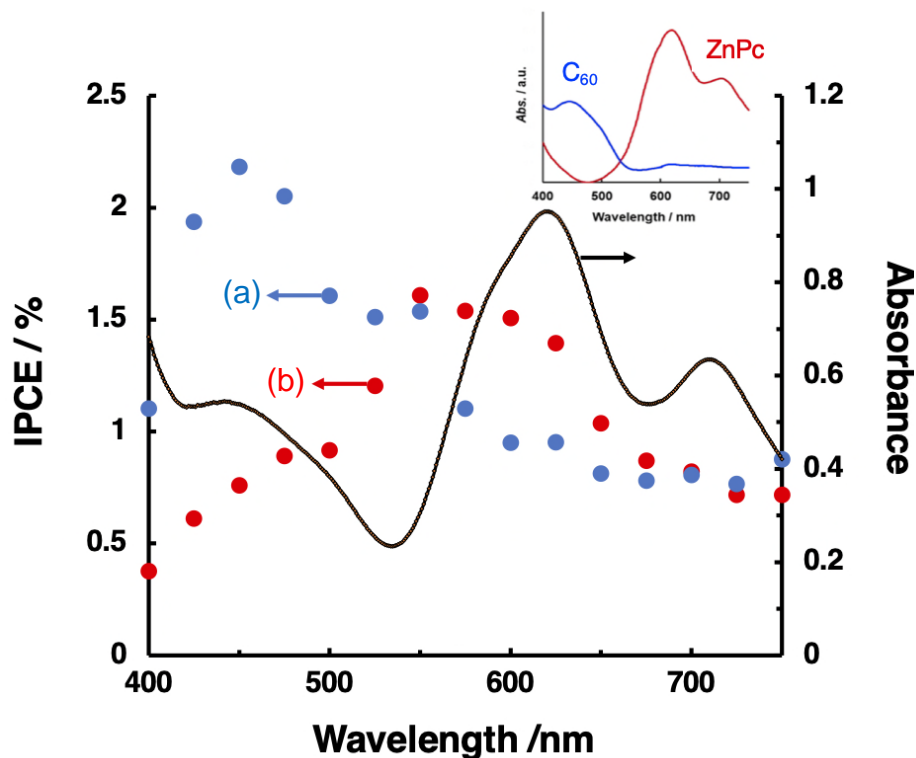
**Figure 3.** Action spectra of ZnPc/$C_{60}$-Au photocurrents obtained under $O_2$ atmosphere. Irradiation was conducted from (a) back side of ITO-coated face and (b) Au-loaded $C_{60}$ surface. Inset shows the absorption spectra of the single-layered ZnPc and $C_{60}$. Film thickness: 75 nm for ZnPc and 125 nm for $C_{60}$; applied potential: 0 V vs. Ag/AgCl; light intensity: 0.2 mW/cm$^2$; electrolyte solution: aqueous $H_2PO_4$ solution (pH = 2).
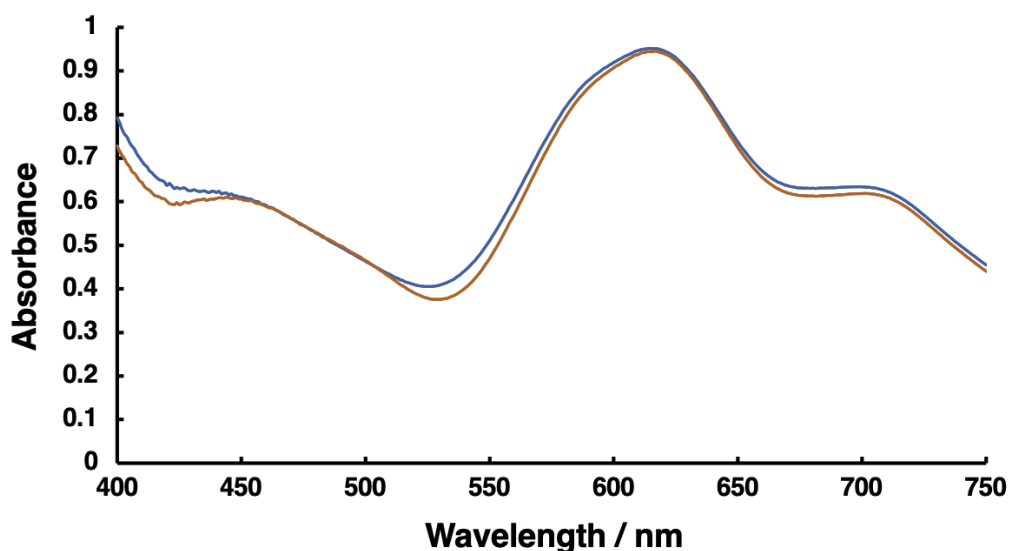


**Figure 4.** Absorption spectra of ZnPc/$C_{60}$-Au before and after $O_2$ reduction.

Comparing **Fig. 2(a)** with a previously reported voltammogram of a BiVO$_4$/Nf[Co$_3$O$_4$] photoanode **[21]**, a potential window, where the photoanodic and photocathodic currents occur simultaneously, was found to be present between +0.2 and +0.4 V (vs. Ag/AgCl). Based on these results,

the photocatalytic system, comprising $ZnPc/C_{60}$-Au and $BiVO_4/Nf[Co_3O_4]$, can be expected to induce the formation of $H_2O_2$ from $H_2O$ and $O_2$ under irradiation.

The photocatalytic formation of $H_2O_2$ was examined according to **Scheme 1**, and the typical data are presented in **Table 1**. It is confirmed that stoichiometric formations of $O_2$ and $H_2O_2$ from $H_2O$ and $O_2$, respectively, occurred successfully, particularly under bias-free conditions (entry 1). Thus, the system demonstrates artificial photosynthesis of $H_2O_2$ in an acidic medium. Furthermore, $H_2O_2$ formation was investigated by applying a bias voltage between the photoelectrodes, and coulometry was simultaneously conducted. The higher the voltage, the larger the amounts of $H_2O_2$ and $O_2$ formed (i.e., the F.E. for the formation of $H_2O_2$ and $O_2$ was always > 90%). The maximum LTH value is approximately 0.007% at 0.2 V (i.e., under the conditions of entry 3). To understand the kinetic characteristics of the present system, control experiments were conducted in the presence of $H_2O_2$ (electron donor) or $Fe^{3+}$ (electron acceptor) at a bias voltage of 0.2 V (**Table 1**). Comparing the present system (entry 3) with the control system with $H_2O_2$ addition (entry 6), it is observed that the amount of $H_2O_2$ formed at the reduction site remains unchanged. However, when $Fe^{3+}$ is added to the electrolyte solution, the amount of $O_2$ increases substantially (entry 7), indicating that $H_2O_2$ formation is the rate-limiting step in the overall reaction.

Photocatalytic $H_2O_2$ formation using the present system can be interpreted as follows: oxidizing and reducing power are generated at $BiVO_4/Nf[Co_3O_4]$ and $ZnPc/C_{60}$-Au, respectively. When only $BiVO_4$ is utilized as the photoanode, it is easy for the photocorrosion of $BiVO_4$ to take place **[31]**. However, as demonstrated in a recent study, the loading of the $Co_3O_4$ co-catalyst on $BiVO_4$ and the ingenious use of the co-catalyst (i.e., $BiVO_4/Nf[Co_3O_4]$) can improve the catalyst stability and efficiently lead to the oxidation of $H_2O$ to $O_2$, even at pH = 2 **[21]**. In addition, our group previously reported that the $ZnPc/C_{60}$ bilayer is an efficient photocathode capable of reducing $H^+$ to $H_2$ in acidic media when Pt is deposited on the $C_{60}$ surface **[22]**. Considering the potentials of $H^+/H_2$ (–0.32 V vs. Ag/AgCl, at pH = 2) and $O_2/H_2O_2$ (+0.38 V vs. Ag/AgCl, at pH = 2), the reduction of $O_2$ to $H_2O_2$ at the $ZnPc/C_{60}$ bilayer is thermodynamically feasible. Thus, the loading of the Au co-catalyst on the $C_{60}$ surface successfully led to the selective formation of $H_2O_2$ from $O_2$. As shown in **Fig. 4**, the absorption spectra of the organo-bilayer remained unchanged before and after $O_2$ reduction, demonstrating the stability of the organo-bilayer during the $H_2O_2$ formation. The low maximal LTH for $H_2O_2$ formation might be due to the deactivation of Au as it dissolved, peeled off, or formed metal oxide. Thus, a novel and active co-catalyst needs to be developed for the rate-limiting $O_2$ reduction. A photoinduced redox reaction generally occurs to originate in oxidation, thus leading to reduction by electrons released through the oxidation reaction. However, in the present system, the electrons generated in $BiVO_4$ filled the holes left in the valence band of ZnPc. This is kinetically more favorable than a system in which electrons generated at the photoanode must participate directly in reduction.

# 4. CONCLUSION

This study presents an example of an artificial photosynthesis system for the formation of $H_2O_2$ in an acidic medium, where $H_2O$ and $O_2$ function as reducing and oxidizing agents, respectively. In the

system comprising $ZnPc/C_{60}$-Au (reduction site) and $BiVO_4/Nf[Co_3O_4]$ (oxidation site), the formation of $H_2O_2$ from $O_2$ occurred stoichiometrically along with the evolution of $O_2$ from $H_2O$, without application of a bias voltage to the system. Although photoelectrochemical conditions, where a bias voltage was applied between the oxidation and reduction sites, were also employed for the formation of $H_2O_2$, a low LTH value (maximum: < 0.01%) was obtained. The results of the control experiments in the presence of $H_2O_2$ (electron donor) or $Fe^{3+}$ (electron acceptor) revealed that rate-limiting $H_2O_2$ formation occurred in the present system. Therefore, an efficient reduction site needs to be developed in terms of both the organo-bilayer and the co-catalyst to improve the system proposed in this study.

**References**

1. H.J. Riedl and G. Pfleiderer, US patent, 2158525 (1939).
2. R. Ciriminna, L. Albanese, F. Meneguzzo and M. Pagliaro, *ChemSusChem,* 9 (2016) 3374.
3. X. Wang, K. Maeda, A. Thomas, K. Takanabe, G. Xin, J. M. Carlsson, K. Domen and M. Antonietti, *Nat. Mater*., 8 (2008) 76.
4. Y. Shiraishi, S. Kanazawa, Y. Kofuji, H. Sakamoto, S. Ichikawa, S. Tanaka and T. Hirai, *Angew. Chem. Int. Ed*., 53 (2014) 13454.
5. W.-C. Hou and Y.-S. Wang, *ACS Sustainable Chem. Eng*., 5 (2017) 2994.
6. Y. Kofuji, Y. Isobe, Y. Shiraishi, H. Sakamoto, S. Ichikawa, S. Tanaka and T. Hirai, *ChemCatChem*, 10 (2018) 2070.
7. L. Zheng, H. Su, J. Zhang, L.S. Walekar, H.V. Molamahmood, B. Zhou, M. Long and Y.H. Hu, *Appl. Catal. B: Environ.*, 239 (2018) 475.
8. L. Zheng, J. Zhang, Y.H. Hu and M. Long, *J. Phys. Chem*. C, 123 (2019) 13693.
9. X. Zeng, Y. Liu, Y. Kang, Q. Li, Y. Xia, Y. Zhu, H. Hou, M.H. Uddin, T.R. Gengenbach, D. Xia, C. Sun, D.T. Mccarthy, A. Deletic, J. Yu and X. Zhang, *ACS Catal*., 10 (2020) 3697.
10. H. Che, X. Gao, J. Chen, J. Hou, Y. Ao and P. Wang, *Angew. Chem. Int. Ed.,* 60 (2021) 25546.
11. C. Pan, G. Bian, Y. Zhang, Y. Lou, Y. Zhang, Y. Dong, J. Xu and Y. Zhu, *Appl. Catal. B: Environ*., 316 (2022) 121675.
12. X. Dong, S. Wu and H. Zhao, *ACS Sustainable Chem. Eng*., 10 (2022) 4161.
13. M. Pourbaix, Atlas of electrochemical equilibria in aqueous solutions, Pregamon Press, (1966) London, UK.
14. Q. Chang, P. Zhang, A.H.B. Mostaghimi, X. Zhao, S.R. Denny, J.H. Lee, H. Gao, Y. Zhang, H.L. Xin, S. Siahrostami, J.G. Chen and Z. Chen, *Nat. Commun*., 11 (2020) 1.
15. Y. Jiang, P. Ni, C. Chen, Y. Lu, P. Yang, B. Kong, A. Fisher and X. Wang, *Adv. Energy Mater*. 8 (2018) 1801909.
16. E.M. Garcia, J.S. Santos, E.C. Pereira and M.B.J.G. Freitas, *J. Power Sources*, 185 (2008) 549.
17. T.W. Kim and K.-S. Choi, *Science*, 343 (2014) 990.
18. JCPDS file 00-044–0081.
19. A. Didehban, M. Zabihi and J. Rahbar-Shahrouzi, *Int. J. Hydrogen Energy*, 45 (2018) 20645.
20. JCPDS file 01-073–1213.
21. T. Murakami, K. Ikezoi, K. Nagai, H. Kato and T. Abe, *ChemElectroChem*, 7 (2020) 5029.
22. T. Abe, Y. Hiyama, K. Fukui, K. Sahashi, K. Nagai, *Int. J. Hydrogen Energy*, 40 (2015) 9165.
23. T. Inasaki and S. Kobayashi, *Electrochem. Acta*, 54 (2009) 4893.

24. J.S. Jirkovský, M. Halasa and D.J. Schiffrin, *Phys. Chem. Chem. Phys.*, 12 (2010) 8042.
25. T. Abe, S. Miyakushi, K. Nagai and T. Norimatsu, *Phys. Chem. Chem. Phys.*, 10 (2008) 1562.
26. M. Zhu, Z. Sun, M. Fujitsuka and T. Majima, *Angew. Chem. Int. Ed.*, 57 (2018) 2160.
27. G. M. Eisenberg, Ind. Eng. *Chem. Anal. Ed.*, 15 (1943) 327.
28. ICSD No. 044362.
29. T. Abe, K. Fukui, Y. Kawai, K. Nagai and H. Kato, *Chem. Commun.*, 52 (2016) 7735.
30. Y. Kawai, K. Nagai and T. Abe, *RSC Adv.*, 7 (2017) 34694.
31. D.K. Lee and K.-S. Choi, *Nat. Energy*, 3 (2018) 53.